Performance of the Adriatic early warning system during the multi-meteotsunami event of 11-19 May 2020: an assessment using energy banners

Iva Tojčić[1*], Cléa Denamiel[1,2], Ivica Vilibić[1]

[1] Institute of Oceanography and Fisheries, Šetalište I. Meštrovića 63, 21000 Split, Croatia
[2] Ruđer Bošković Institute, Division for Marine and Environmental Research, Bijenička cesta 54, 10000 Zagreb, Croatia

Correspondence to: I. Tojčić, (tojcic@izor.hr)

Abstract. This study quantifies the performance of the Croatian meteotsunami early warning system (CMeEWS) composed of a network of air pressure and sea level observations, a high-resolution atmosphere-ocean modelling suite and a stochastic surrogate model. The CMeEWS, which is not operational due to a lack of numerical resources, is used retroactively to reproduce the multiple events observed in the eastern Adriatic between the 11th and 19th of May 2020. The performances of the CMeEWS deterministic models are then assessed with an innovative method using energy banners based on temporal and spatial spectral analysis of the high-pass filtered air pressure and sea-level fields. It is found that deterministic simulations largely fail to forecast these extreme events at endangered locations along the Croatian cost mostly due to a systematic north-westward shift of the atmospheric disturbances. Additionally, the use of combined ocean and atmospheric model results, instead of atmospheric model results only, is not found to improve the selection of the transects used to extract the atmospheric parameters feeding the stochastic meteotsunami surrogate model. Finally, in operational mode, the stochastic surrogate model would have triggered the warnings for most of the observed events, but also setting off some false alarms. Due to the uncertainties associated with operational modelling of meteotsunamigenic disturbances, the stochastic approach has thus proven to overcome the failures of the deterministic forecasts and should be further developed.

1 Introduction

Atmospherically-driven extreme sea-levels (e.g. wind storms, hurricanes), associated with flooding producing substantial damages to houses, goods, and infrastructures, are among the main hazards impacting the coastal communities (Nicholls and
25 Cazenave, 2010; Neumann et al., al., 2015). As such, meteorological tsunamis (commonly referred as meteotsunamis) are sea-level oscillations with characteristics similar to seismic or landslide tsunamis but generated by atmospheric gravity waves, frontal passages, pressure jumps, squalls, etc., though a multi-resonant mechanism (Monserrat et al., 2006). The principal generation mechanisms are the open-ocean resonance occurring between the ocean and the air pressure oscillations at time scales ranging from a few minutes to a few hours (e.g. Proudman, 1929), as well as the coastal amplification that includes also
30 so-called harbour resonance (Miles and Munk, 1961; Rabinovich, 2009). Locally they can be destructive, not only due to extreme sea-levels (Hibiya and Kajiura, 1982; Salaree et al., 2018), but also to dangerous currents in constrictions or in coastal zone (Ewing et al., 1954; Vilibić et al., 2004; Linares et al., 2019). The strongest meteotsunami on record in the Mediterranean Sea hit Vela Luka, Croatia, in June 1978, with a wave height of 6 m (crest-to-trough) and a period of 18 min. The meteotsunami lasted several hours and caused 7 million US dollar damages (Vučetić et al., 2009; Orlić et al., 2010).

35 In certain locations around the world, due to a combination of weather patterns, geography and bathymetry, meteotsunamis can be a regularly occurring phenomenon. The Balearic Islands and Croatian coastline in the Mediterranean Sea, a few od Japan's gulfs and bays, the Great Lakes and the US East Coast, western Australian coastline are good examples (Pattiaratchi and Wijeratne, 2015; Rabinovich, 2020). Meteotsunami early warning systems, helping the local population to prepare for these destructive events, are thus important for the coastal communities living in such places. Vilibić et al. (2016) pointed out
40 that meteotsunami early warning systems can be created based on the four approaches: (1) identification of tsunamigenic atmospheric synoptic conditions; (2) real-time detection of tsunamigenic atmospheric disturbances using a microbarograph network; (3) measurement and tracking of high-frequency sea-level oscillations by high-resolution digital tide gauges; and (4) numerical simulation of meteotsunamis based on coupling of atmosphere-ocean numerical models. As it stands today, the only fully operational meteotsunami early warning system in the world is located in the Balearic Islands. It is based on forecasts
45 given both at a qualitative level with the identification of favourable synoptic conditions a few days ahead (Jansà et al., 2007; Jansà and Ramis, 2020) and with the deterministic results of the operational BRIFS (Balearic Rissaga Forecasting System, www.socib.eu) model (Renault et al., 2011). In the United States, meteotsunami early warning systems are still under development by the NOAA (National Oceanic and Atmospheric Administration) and will be based on high-resolution air pressure measurements combined with forecast models (Anderson et al., 2020). Finally, the recently developed Croatian
50 Meteotsunami Early Warning System (CMeEWS) is based on an observational network of pressure sensors and tide gauges, as well as on the deterministic AdriSC modelling suite (Denamiel et al., 2019a) and the stochastic meteotsunami surrogate model (Denamiel et al., 2019b, 2020). It provides meteotsunami hazard assessments depending on forecasted and measured

air pressure disturbances but is, unfortunately, not used operationally since November 2019 due to a lack of high-performance computing resources needed to execute in real-time such numerically demanding suite.

55   However, the CMeEWS applications to recent meteotsunami events may surely be used to better quantify its reliability and to improve its performance. Recently, an exceptional multi-meteotsunami event, that lasted for a week between the 11th and 19th of May 2020, occurred in the Croatian cities of Vela Luka (VL), Stari Grad (SG) and Vrboska (Vr), located along the coasts of the Dalmatian islands in the Adriatic Sea (Fig. 1). Therefore, the deterministic and stochastic AdriSC models have been run retroactively in operational (hindcast) mode (i.e. in the exact same conditions than the daily meteotsunami forecasts would

60   have been produced operationally) for this 11-19 May 2020 period. As quoted by Denamiel et al. (2020), forecasting the right speed and frequency (period) of the travelling atmospheric disturbances is crucial for meteotsunami hazard assessments in the harbours of Vela Luka, Stari Grad and Vrboska. Therefore, unlike previous studies on the performances of the CMeEWS operational models, this analysis introduces the novelty of using energy banners – based on the spectral analysis of the high-pass filtered air pressure and sea-level fields – as a tool to evaluate the capacity of the AdriSC deterministic model to reproduce

65   the frequency of the meteotsunamigenic disturbances measured during the 11-19 May 2020 period. The presented work introduces the CMeEWS (including the AdriSC modelling suite, the stochastic surrogate model and the observational network) in Sect. 2. Section 3 describes the 11-19 May 2020 multi meteotsunami event, using eyewitness reports, available observations and reanalysis products. Sect. 4 provides the verification of the AdriSC deterministic model, while Sect. 5 presents the main results of the study – i.e. the meteotsunami energy banners – that are used to detect the strongest atmospheric disturbances.

70   Then, the stochastic meteotsunami hazard assessments, based on variables extracted using the selected energy banners, are presented in Sect. 6. Finally, the findings of this study are summarized in Sect. 7.

2 The Croatian Meteotsunami Early Warning System

The Croatian Meteotsunami Early Warning System (CMeWS) receives three different kind of data: (1) high-resolution atmospheric and ocean model results provided by the Adriatic Sea and Coast (AdriSC) modelling suite (Denamiel et al.,

75   2019a), (2) measurements from the MESSI (www.izor.hr/messi) observational network along the Adriatic coast and (3) meteotsunami hazard assessments based on the stochastically estimated maximum elevation distributions derived from a meteotsunami surrogate model (Denamiel et al., 2019b, 2020).

2.1 AdriSC modelling suite

The AdriSC modelling suite is composed of a basic module providing kilometre-scale atmospheric and ocean circulation over

80   the entire Adriatic region, forcing a dedicated meteotsunami module (Denamiel et al., 2019a). The basic module uses a modified version of the Coupled Ocean-Atmosphere-Wave-Sediment-Transport (COAWST) modelling system developed by Warner et al. (2010). The dedicated meteotsunami module couples offline the Weather Research and Forecasting (WRF) model (Skamarock et al., 2005) – which downscales the hourly results of the basic module to a 1.5-km resolution for a grid covering

the entire Adriatic Sea – with the 2DDI ADvanced CIRCulation (ADCIRC) model (Luettich et al., 1991), using a mesh of up
85   to 10 m in resolution in the areas sensitive to meteotsunami hazard. In this deterministic configuration, the ADCIRC model is
forced every minute by the WRF 1.5-km wind and pressure fields, and every hour by the basic module sea-level fields
(including tides).
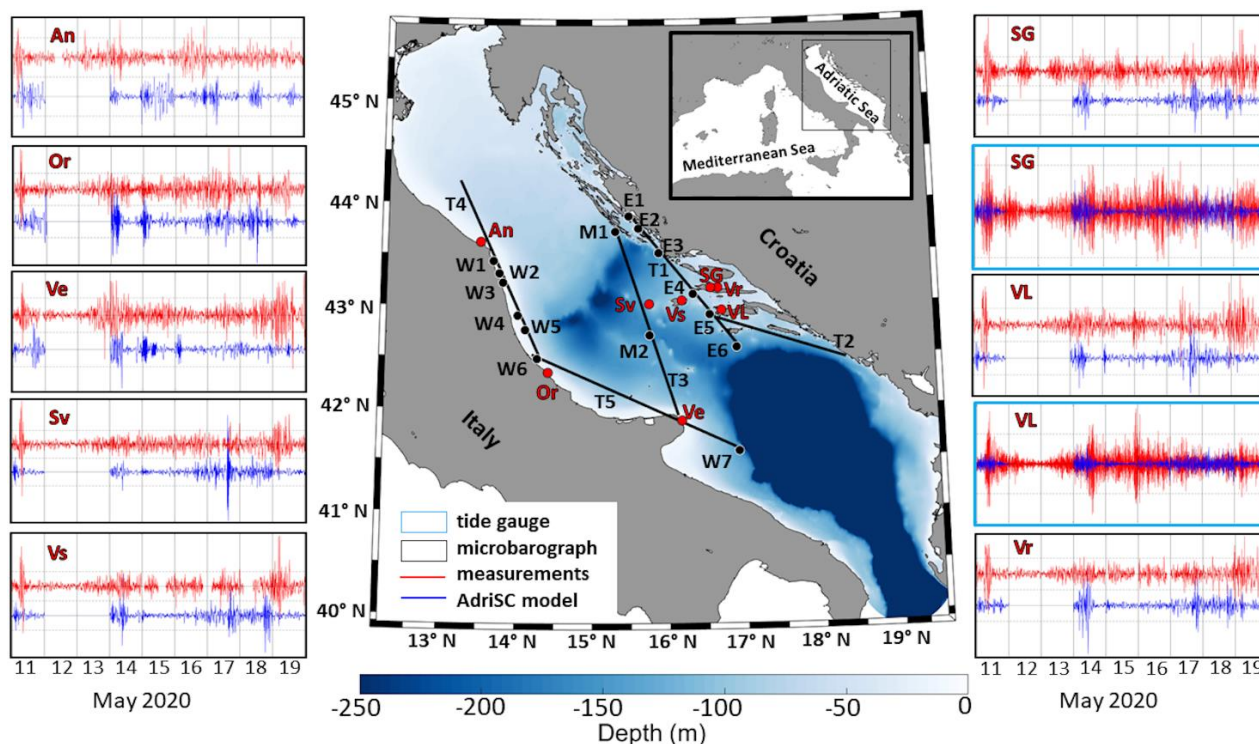
Figure 1: Bathymetry of the Adriatic Sea (centre panel), with positions of microbarographs and tide gauges (red circles). Black
90   **circles denote model grid points along transects T1 to T5 (black lines) on which the highest energy is reproduced within selected**
meteotsunami energy banners in the eastern (E1 to E6), middle (M1 and M2) and western (W1 to W7) Adriatic. Left and right
panels display observed (in red) and modelled (in blue) high-pass filtered time series of air pressure (black rectangles) and sea-level
(blue rectangles) during the 11-19 May 2020 period. Distance between adjacent horizontal grid lines (dashed) stands for 1.0 hPa in
air pressure, as well as 0.25 m and 0.5 m in sea-level for Stari Grad and Vela Luka, respectively.

95   In operational mode (Denamiel et al., 2019a, 2019b) the AdriSC modelling suite runs every day with the basic module initial
state and boundary conditions provided by (1) the previous day 12 UTC based analysis of the ECMWF 10-day forecast model
(HRES at 0.1° resolution; Zsótér et al., 2014) for the atmosphere and (2) the Mediterranean Forecasting System
(MFS/MEDSEA at 1/24° resolution; Pinardi et al., 2003) for the ocean. At midnight, the next 48 h hourly-forecast results from
the basic module, as well as the 15 min-forecast results from the meteotsunami module for the next day, are published at
100   http://www.izor.hr/adrisc. However, since November 2019, the operational AdriSC model component has been interrupted
due to a lack of numerical resources and no daily forecast is anymore published.

In this study, in order to evaluate the capacity of the CMeEWS to provide meaningful meteotsunami hazard assessments, the AdriSC modelling suite is run in operational (hindcast) mode after the 11-19 May 2020 multi-meteotsunami event took place. This means that the 10-day forecasts derived with the ECMWF HRES and MEDSEA/MSF models on the 8th, 9th, 10th, ..., 16th

105   of May 2020 are used to hindcast the meteotsunamigenic conditions of the 11th, 12th, 13th, ..., 19th of May 2020. However, as no meteotsunamigenic disturbances were recorded during the 12th and 13th May (Fig. 1), these two days are not simulated in order to spare some numerical resources. All the results presented hereafter are thus extracted from the WRF 1.5-km model in the atmosphere and the ADCIRC unstructured model in the ocean.

2.2 Observational network

110   The MESSI observational network consists of eight microbarographs, with an accuracy of 0.01 hPa, and two tide gauges, all setup with a 1-min sampling rate and listed in Table 1. Microbarographs are installed in areas where either the generation or the amplification of meteotsunamis are known to occur (red circles, Fig. 1): Ancona (An), Ortona (Or), and Vieste (Ve) located along the western Adriatic coast, Vis (Vs) and Svetac (Sv) in the middle of the Adriatic Sea, and Vela Luka (VL), Stari Grad (SG) and Vrboska (Vr) on the eastern Adriatic coast. Tide gauges are located in Vela Luka (VL) and Stari Grad (SG), which

115   are known to be harbours sensitive to meteotsunamis (red circles, Fig. 1). However, one should be aware that the tide gauges are located not at the tops of the affected bays that are normally most affected by meteotsunamis, but about 2 km for the tops, thus the observed high-frequency sea level oscillations at tide gauges are 2 to 3 times lower than reported by eyewitnesses at the bays' tops.

Table 1. Microbarograph and tide gauge locations.

Location	Coordinates	Area	Observations
Ancona (An)	13.506 °E 43.625 °N	Western Adriatic	air pressure
Ortona (Or)	14.415 °E 42.356 °N	Western Adriatic	air pressure
Vieste (Ve)	16.177 °E 41.888 °N	Western Adriatic	air pressure
Svetac (Sv)	15.757 °E 43.024 °N	Middle Adriatic	air pressure
Vis (Vs)	16.192 °E 43.057 °N	Middle Adriatic	air pressure
Stari Grad (SG)	16.576 °E 43.180 °N	Eastern Adriatic	air pressure & sea-level
Vela Luka (VL)	16.718 °E 42.962 °N	Eastern Adriatic	air pressure & sea-level
Vrboska (Vr)	16.672 °E 43.181 °N	Eastern Adriatic	air pressure

120

2.3 Stochastic surrogate model

Uncertainties linked to the deterministic forecast of the location, direction, amplitude, speed, period and width of the atmospheric disturbances driving meteotsunami events in the Adriatic Sea are known to be quite large (Belušić et al.., 2007; Šepić et al., 2009; Denamiel et al., 2019a). In other words, it is unlikely for atmospheric deterministic models to forecast
125 meteotsunamigenic disturbances with proper speed and period and at the right location. Consequently, deterministic ocean models often fail to reproduce or underestimate the meteotsunami events in sensitive harbours (e.g. Vela Luka, Stari Grad and Vrboska). To bridge such a problem, the meteotsunami stochastic surrogate model, used to propagate the uncertainties of the atmospheric disturbances to the meteotsunami waves, was thus developed within the CMeEWS (Denamiel et al., 2019b, 2020). This model is optimizing a great number of ADCIRC simulations via a generalized Polynomial Chaos expansion (gPCE)
130 method (Xiu and Karniadakis, 2002; Soize and Ghanem, 2004), where a particular simulation is forced by synthetic air pressure fields depending on six stochastic parameters: start location ($y0$), direction (θ), speed (c), period (T), amplitude (PA), and width (d) of the disturbance (Denamiel et al., 2018). These six parameters are assumed to have uniform distributions and are adapted to the middle Adriatic meteotsunamis on the following intervals: $y0 \in$ [41.25° N, 43.65° N], $\theta \in [-\pi/3, \pi/2]$, $c \in$ [15 m s^{-1}, 40 m s^{-1}], $T \in$ [300 s, 1800 s], PA $\in$ [0.5 hPa, 4 hPa], and $d \in$ [30 km, 150 km].

135 Within the CMeEWS, the ranges of the stochastic parameters used as input to the surrogate model are extracted from the forecasted WRF 1.5-km high-pass filtered air pressure results, adding the uncertainty of ±0.24° N for latitude of origin, ±0.26 rad for direction of propagation, ±0.35 hPa for amplitude, ±150 s for period, and ±12 km for width, following the values determined by Denamiel et al. (2019b). For each sensitive location along the Croatian coast, the output of the surrogate model consists in the distribution of maximum elevations produced with 20 000 random combinations of the input parameters selected
140 within the defined ranges. Additionally, to provide a meteotsunami hazard assessment derived from the surrogate model, Denamiel et al. (2019b) prescribed a flooding threshold – defined as the maximum elevation above which flooding would occur – considering the resilience of the coastline at the different sensitive locations. For Vela Luka, Stari Grad and Vrboska, these thresholds are defined as 1.05 m, 0.45 m and 0.55 m respectively. In operational mode, the meteotsunami warning is triggered when the probability of crossing the flooding threshold (derived from the maximum elevation distributions provided
145 as the surrogate model output) is above or equal to 10 %.

3 Description of the event and background analysis

This long-lasting meteotsunami event was indeed reported by media, in particular by eyewitnesses in Vrboska with two YouTube videos (https://www.youtube.com/watch?v=vz9G5E9ravc; https://www.youtube.com/watch?v=-aD9q4QMANE) and by local web portals in Vela Luka and Stari Grad. In particular, Dalmacija danas (https://www.dalmacijadanas.hr/) wrote
150 on the 14th of May: "Changes in air pressure have a pronounced effect on the sea-level in the Adriatic, which is most noticeable on the Dalmatian islands in the last two days. There is a constant change in sea-level throughout the day, and today it was most pronounced in the afternoon in Vela Luka. […] the sea-level fluctuated in the range of about 70 centimetres. The sea rose and

flooded the waterfront, then receded abruptly, leaving the boats dry. The phenomenon was also recorded on Hvar, for example in Stari Grad, but it was less pronounced." On May 16th another local web portal, Morski.hr, published an article titled

155 "Meteotsunami in Vela Luka: The sea is pouring into shops and cafes. This has been going on for three days now!" with the testimony of a local, Ljubo Padovan: "This is something we haven't had in years and it has been going on for full three days. The sea got into some shops and cafes again. When the sea recedes, one can walk from one side of the bay to the other. The sea flooded everything again last night. The situation is not calming down even after three days, that is very unusual."

Concerning the observations (Fig. 1), on the 11th of May intense high-frequency sea-level oscillations reach up to 80 cm of

160 height (crest-to-trough) and 16 min period at 9:40 UTC in Vela Luka as well as 53 cm of height and 18 min of period at 11:07 UTC in Stari Grad. Additionally, all microbarographs record an intensification of the air pressure oscillations, with a maximum high-frequency amplitude of 3.1 hPa and period of a 13 min documented for Vela Luka. Air pressure oscillations calm down on May 12th and 13th but, following reported flooding, increase again on May 14th, especially in Ancona and Vieste. On this day, in Vela Luka, air pressure oscillations are about 2 times weaker than on the 11th but the height of sea-level oscillations

165 almost reaches 80 cm with a 15 min period. However, in Stari Grad, sea-levels oscillate between -25 and 25 cm from 8:00 UTC to 16:00 UTC. Even though the sea-level oscillations in Stari Grad harbour are two times smaller than during the 11th of May, flooding still occurred probably due to the additional effects of tidal elevation and/or storm surge. Lower intensity oscillations of both air pressure and sea-level follow the next days until around midnight on the 16th of May, when another meteotsunami event takes place. For this event, air pressure oscillations are unusually low, even in Ancona which records the

170 strongest ones. However, in Vela Luka the height of the sea-level oscillations goes up to 80 cm with a 13 min period. Despite the reports of flooding in Stari Grad, identically to the 14th of May, the sea-levels only oscillate between -25 and 25 cm. The pressure oscillations do not completely vanish in the following days and on the 19th of May strong air pressure disturbances with heights of above 2.5 hPa occur in Svetac, Vieste, Vis, Vrboska and Vela Luka. However, no flooding is recorded in Vela Luka nor Stari Grad where the recorded sea-level oscillations do not surpass 30 cm and 20 cm respectively.

175 The synoptic conditions over Europe derived from ERA5 reanalysis (Hersbach et al., 2020) – temperature at 850 hPa, winds at 500 hPa and mean sea-level air pressure (Fig. 2) – are extracted at times close to the flooding of Vela Luka, Stari Grad and Vrboska harbours: in the morning of the 11th of May, around midday on May 14th and around midnight on May 16th. For all the flooding events, the conditions show the advection of warm air from the Sahara towards the Adriatic at 850 hPa, associated with strong south-westerly winds at 500 hPa with speeds over 30 m s^{-1}. Additionally, the mean sea-level air pressure over the

180 Adriatic indicate either a trough stretching from the north Europe, as on the 11th, or a cyclone, deeper on the 14th of May and quite weak on the 16th of May. These synoptic conditions are known to occur during the Mediterranean meteotsunamis (Jansá et al., 2007; Vilibić et al., 2008; Šepić et al., 2012, 2015), where atmospheric disturbances (particularly atmospheric gravity waves) can be generated along the strong frontal gradients of the jet-streams as seen in Fig. 2 and propagate over long distances in the form of so-called ducted waves (Lindzen and Tung, 1976; Monserrat and Thorpe, 1996).
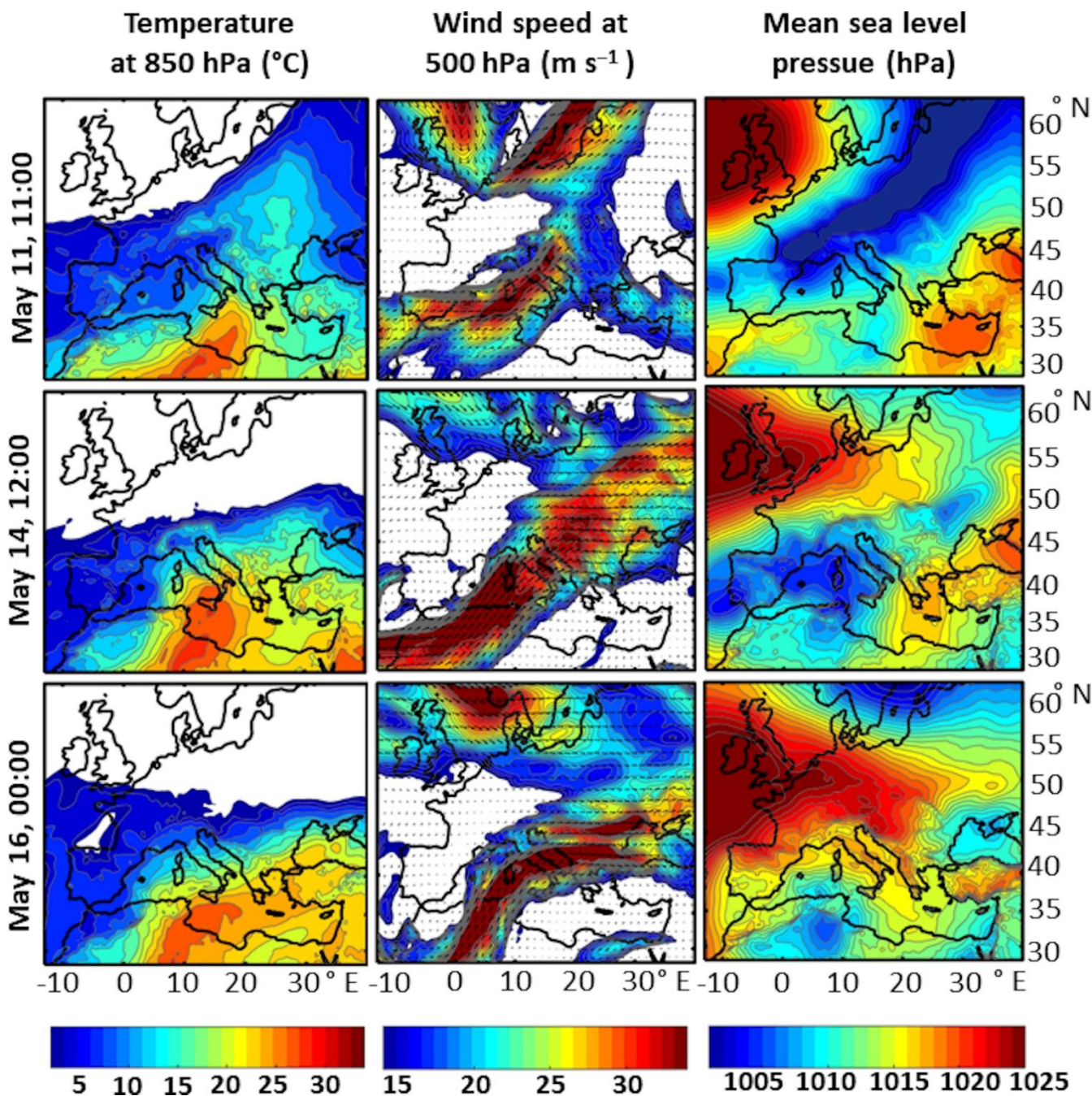
Figure 2: Synoptic settings over Europe – temperature at 850 hPa (left panels), winds at 500 hPa (middle panels) and mean sea-level pressure (right panels) – extracted from ERA5 reanalysis at times closest to the flooding in Vela Luka, Stari Grad and Vrboska harbours.

4 Verification of modelled meteotsunamigenic disturbances

190   At a very basic level, a direct comparison of modelled and measured high-pass filtered air pressure and sea-level time series
(Fig. 1) is used to assess the capacity of the AdriSC deterministic model to reproduce the meteotsunami events at the observing
stations during the 11-19 May 2020 period. The events on the 11th and 16th of May are completely missed by both the WRF
1.5-km and ADCIRC models. However, the meteotsunami event of the 14th of May is partially captured by the AdriSC model.
Air pressure oscillations are indeed simulated in Vieste, Vis, Stari Grad, Vela Luka and Vrboska, along with weaker than

195   measured sea-level oscillations in Stari Grad and Vela Luka. AdriSC model results for the 17th of May are generally in
accordance with the measurements, with underestimated pressure and sea-level oscillations in Ortona, Stari Grad and Vela
Luka and overestimated pressure oscillations in Svetac.
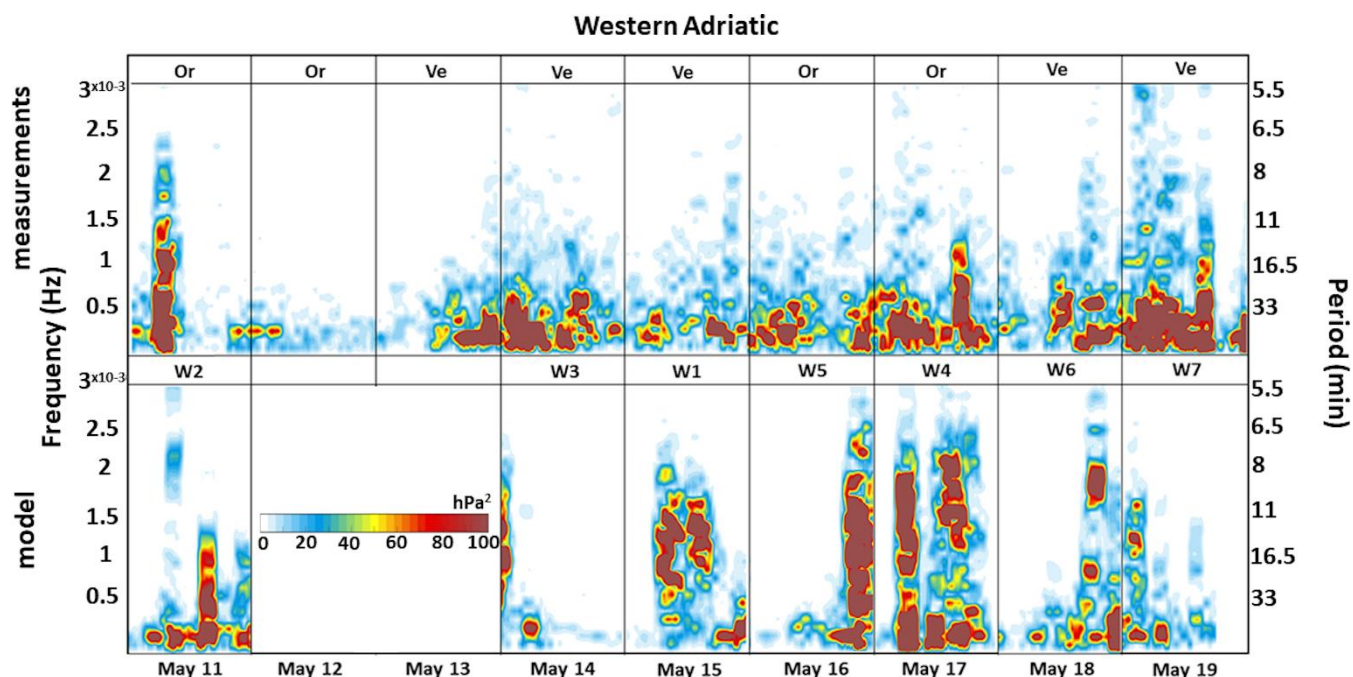
Figure 3: Modelled and measured composites of high-pass filtered air pressure frequency-time spectrograms for the western
200   **Adriatic region. Maximum daily energies measured by the microbarographs (observed composite) and modelled at one WRF 1.5-**
km model grid point (modelled composite) are collocated.

Even though the deterministic AdriSC model fails to forecast two of the three observed meteotsunami events, the event mode
(i.e. meteotsunamis may occur) of the CMeEWS is triggered for all the days of the 11-19 May 2020 period (except the 12th
and 13th when model results are not available). Following Denamiel et al. (2019b), the event mode is triggered when the spatial
205   coverage of the maximum temporal rate of change of the high-pass filtered air pressure, derived at each WRF 1.5-km grid sea
point, are greater than 5 % (Fig. S1 provided as supplementary material). This implies that the AdriSC WRF 1.5-km model is

capable to reproduce strong meteotsunamigenic disturbances over the Adriatic Sea for all days in which meteotsunamis has been observed, yet probably having an offset to locations of endangered bays to the atmospheric disturbance banners.

Measured and modelled composites of air pressure frequency-time spectrograms in the eastern, middle and western Adriatic
210 Sea (Fig. 3 to 5) are thus used to compare the energy content of the meteotsunamigenic disturbances as observed by the microbarographs and forecasted with the WRF 1.5-km model along the disturbance trajectories (banners), here represented by grid points W1-W7, M1-M2 and E1-E6, in addition to grid points next to microbarograph stations. The spectral composites are (1) estimated separately for each day, based on the measured and day-by-day operationally forecasted 1-min air pressure series at the location of interest, and (2) containing running spectra over a day, estimated every 30 min and over 12 h period
215 cantered at the time of interest. Overall, no pronounced energy peaks are found in the spectrograms, which is typical for spectra of intense air pressure characterized by a number of oscillatory movements with no dominant period (Monserrat and Thorpe, 1992; Šepić et al., 2012; Zemunik et al., 2020). Additionally, in operational mode, the CMeEWS would have provided warnings for a full day (next 30-h period including night hours pass midnight) and not for a precise time. It thus may be noticed that, despite this analysis being temporal, discussions about the differences between modelled and measured timing of the
220 meteotsunami events are not relevant for the model verification.

For the 11th of May, the highest energies from the observed composite are located at Or with frequencies below 1.5 10-3 Hz (11 min period) and around 1.8 10-3 Hz (9.25 min period) for the western Adriatic region, at Sv with frequencies below 1.0 10-3 Hz (16.5 min period) for the middle Adriatic region, and at VL with frequencies below 1.1 10-3 Hz (15 min period) as well as with the 1.4 10-3 Hz (12 min) and 1.9 10-3 Hz (8.8 min) frequencies for the eastern Adriatic region. For this event, the
225 WRF 1.5-km model produces at E1 located far northwest from Vela Luka substantially lower energies at the same frequencies than the observed composite, but with high energies at frequencies up to 1.1 10-3 Hz (15 min period) in the western Adriatic, up to 0.8 10-3 Hz (20.8 min period) in the middle Adriatic and at 1.0 10-3 Hz (16.5 min period). This implies that the modelled atmospheric disturbances are less energetic and located further north compare to the observed ones.

During the calm period between the 12th and 13th of May, the energy of the observed spectrograms is much lower than during
230 the meteotsunami events.

However, on the 14th of May, the highest energy values from the observed composite are found at Ve with frequencies below 0.7 10-3 Hz (24 min period) for the western Adriatic region, at Vs with frequencies below 0.55 10-3 Hz (30 min period) for the middle Adriatic region, and at SG with frequencies below 0.5 10-3 Hz (33 min period) for the eastern Adriatic region. The highest energies simulated by the model are located at W3 with frequencies up to 1.8 10-3 Hz (9.25 min period) for the western
235 Adriatic region, at Vs with frequencies up to 1.1 10-3 Hz (15 min period) for the middle Adriatic region, and at E6 located south from Stari Grad with frequencies up to 1.5 10-3 Hz (11 min period) for the eastern Adriatic region. It is unlikely that the modelled atmospheric disturbance can travel from W3 to E6 by crossing diagonally the middle Adriatic region. The results are thus probably coming from more-than-one atmospheric disturbances that occurred during the 14th of May and changed their energies when crossing the Adriatic.
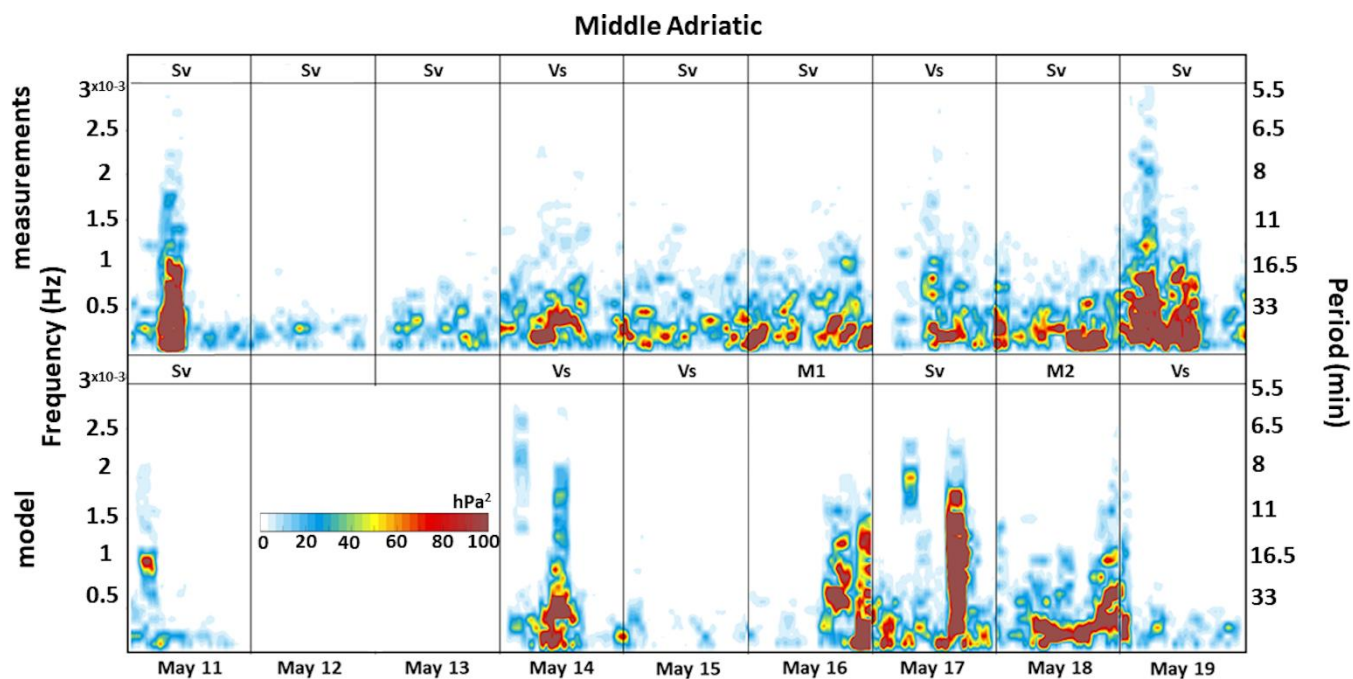
240

Figure 4: As in Fig. 3, but for the middle Adriatic region.

For the 15th and 16th of May, the energies of the observed composite are higher than during the calm background period (between the 12th and 13th of May), but lower than during the meteotsunami events. For the 15th of May, the model produces high energies at frequencies up to 2.0 10-3 Hz (8 min period) at W1 in the western Adriatic region. However, this disturbance

245 does not propagate to the east as the spectrograms in the middle and eastern Adriatic regions have extremely low energy. Energy in the model for the 16th of May is negligible in the western Adriatic region, but for the middle and eastern Adriatic regions high energies at frequencies below 1.5 10-3 Hz are found at M1 and E2, respectively. In other words, even though the meteotsunami event of the 16th of May is missed by the AdriSC model (Fig. 1), the WRF 1.5-km model simulates a strong meteotsunamigenic disturbance shifted north-westward compared to the observations.

250 On the 17th of May the highest energies from the observed composite are located at Or for the western Adriatic region, at Vs for the middle Adriatic region and at SG for the eastern Adriatic region. High energies are also found in the modelled composite at up to 2.2 10-3 Hz (7.5 min period) at W4 for the western Adriatic region, up to 1.8 10-3 Hz (9 min) at Sv for the middle Adriatic region, and up to 1.0 10-3 Hz (16.5 min period) at E5 for the eastern Adriatic region. The spatial layout of the highest energy points again illustrates the limitations of the applied methodology when multiple disturbances are simulated.

255 Nevertheless, obtained results imply that the different disturbances in the model are more energetic than the one observed by the microbarographs.
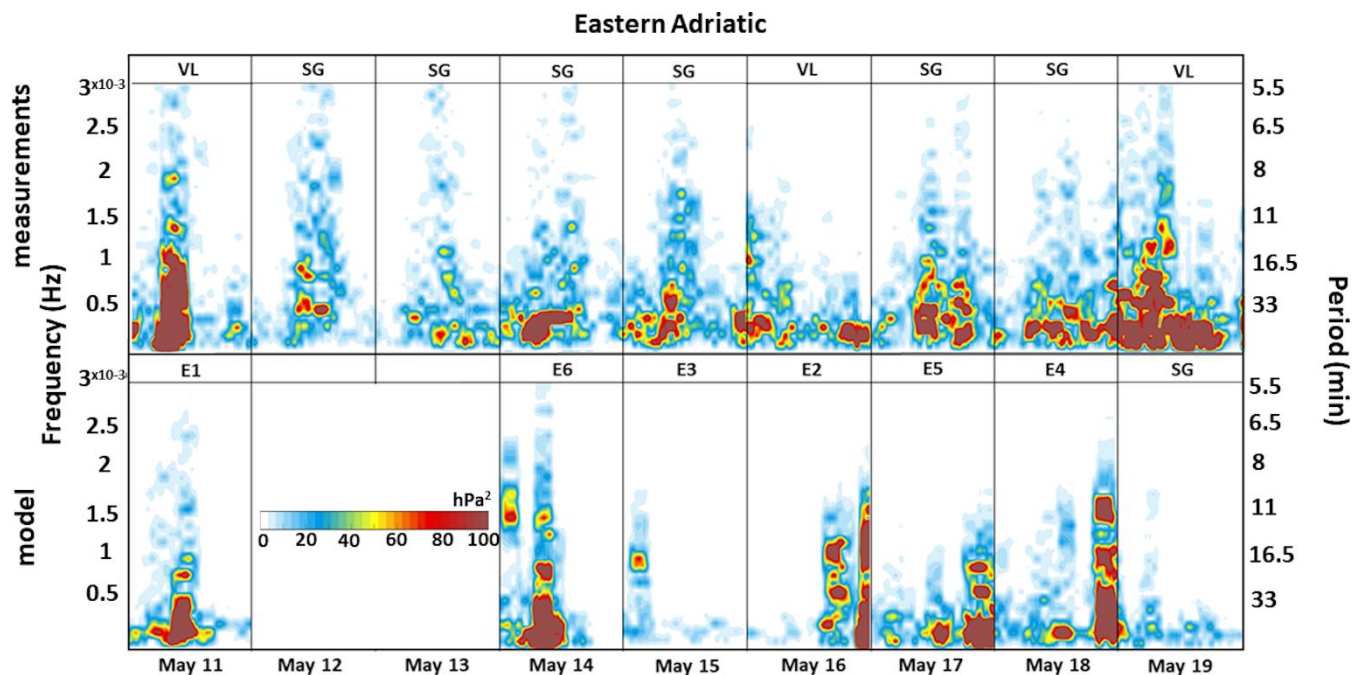
Figure 5: As in Fig. 3, but for the eastern Adriatic region.

More energy is found in the observed spectrograms for the 18th of May than during the calm background period, but less than
260 during the meteotsunami events. The model, however, produces high energies at high-frequencies of about 2.0 10-3 Hz (8 min
period) at W6 for the western Adriatic region and 1.75 10-3 Hz (9.5 min period) at E4 for the eastern Adriatic region.
Atmospheric disturbance energy at M2 is the highest for middle Adriatic region than for the western and the eastern Adriatic
regions, particularly for lower frequencies.

Conditions are again more energetic on the 19th of May, with highest energies in the observed composite at frequencies up to
265 1.5 10-3 Hz (11 min period) at Ve and VL, and up to 1.25 10-3 Hz (13 min period) at Sv. The model fails to reproduce these
disturbances and only simulates high energies at W7, in the southernmost point of the studied area.

In brief, periods between 10 min and 20 min – typical of meteotsunamigenic disturbances – are found to often occur in the
analysis of the frequency-time spectrogram composites (Figs. 3 to 5). Additionally, systematic biases exist in the forecasted
atmospheric disturbances, as often simulated further northwest than the observed ones. Finally, this analysis has demonstrated
270 that the Adriatic high-frequency sea-level oscillations of 11-19 May 2020 are induced by atmospheric forcing of diverse spatial
and temporal characteristics.

5 Meteotsunami energy banners

Given the lack of reliability of the deterministic AdriSC model to properly forecast spatial and temporal characteristics of the
multi-meteotsunami event of the 11-19 May 2020 period, the warnings released by the CMeEWS would have fully rely on the
results of the stochastic surrogate model forced with input parameters extracted from the WRF 1.5-km simulations. The values
of the six stochastic parameters – which serve as input of the stochastic surrogate model – are indeed derived from the modelled
meteotsunamigenic disturbances. The meteotsunami energy banners including their impact to the ocean are thus documented
along the selected transects where these parameters are extracted. The approach used to select these transects and analyse the
meteotsunami energy banners is presented below:

(1) the spatial variances of the WRF 1.5-km high-pass filtered air pressure results are calculated on a 3-hour interval
(i.e. 8 time-windows per day),

(2) the transects describing the meteotsunami energy banner are selected, from all the time windows derived during
the 11-19 May 2020 period, along the paths with highest variances,

(3) spectrograms of the modelled high-pass filtered air pressure and sea-level results over the selected transects are
computed on the same 3-hour interval as used for the variance estimations.

Along these transects, the Proudman resonance is likely to occur for Froude number (Fr) ranging from 0.9 and 1.1 (i.e. when
the speed of the atmospheric disturbance v is matching the speed of the long ocean waves $C = \sqrt{gH}$, with g the gravitational
acceleration and H the local depth, Šepić et al., 2015). The speeds of the tracked atmospheric disturbances along the transects
are thus determined by analysing the WRF 1.5-km high-pass filtered air pressure time series through following propagation of
the strongest disturbance peaks. Then, the depths at which the Proudman resonance would have been likely to occur for each
transect are inferred.

Additionally, a new variable is introduced, referred hereafter as transect sampling criteria and consisting in multiplying the
spatial variances of the high-pass filtered air pressure and sea-level model results estimated on a 3-hour interval. The transect
sampling criteria tends to zero when there is no ocean response to the atmospheric forcing, i.e. when no resonant transfer of
energy from the atmosphere to the sea is occurring. It should be noted that such a criterion could not be directly derived from
the sea-level variance, which provides a noisy and mostly untraceable signal due to the numerous interactions of the ocean
waves with the bathymetry including, for example, the reflection and refraction around the islands.

The air pressure variance, the transect sampling criteria and spectrograms along the most energetic transects (following the air
pressure variance) during the 11-19 May 2020 period are displayed in Figs. 6 to 10 and in supplementary material (Figs. S2 to
S15). The figures also mark the sections of the transect where the speed of atmospheric disturbance is estimated and where the
Proudman resonance is likely to occur (i.e. where 0.9 < Fr < 1.1). For the 11th of May, the modelled air pressure variances
(Figs. 6, S2 and S3, left top panel) and the associated transect sampling criteria (Figs. 6, S2 and S3, right top panel) are
indicating maximum meteotsunami energy banners located far too northwest from Vela Luka, Vrboska and Stari Grad
harbours, where the meteotsunami event is observed. Nevertheless, atmosphere over the two selected transects is highly

energetic and the pronounced disturbances are travelling with a speed between 12.5 m s−1 and 33.32 m s−1 over relatively

shallow areas. Despite the Proudman resonance being possible over a large section of the transects, the energy transferred to

the ocean is not substantial anywhere but near the coast.
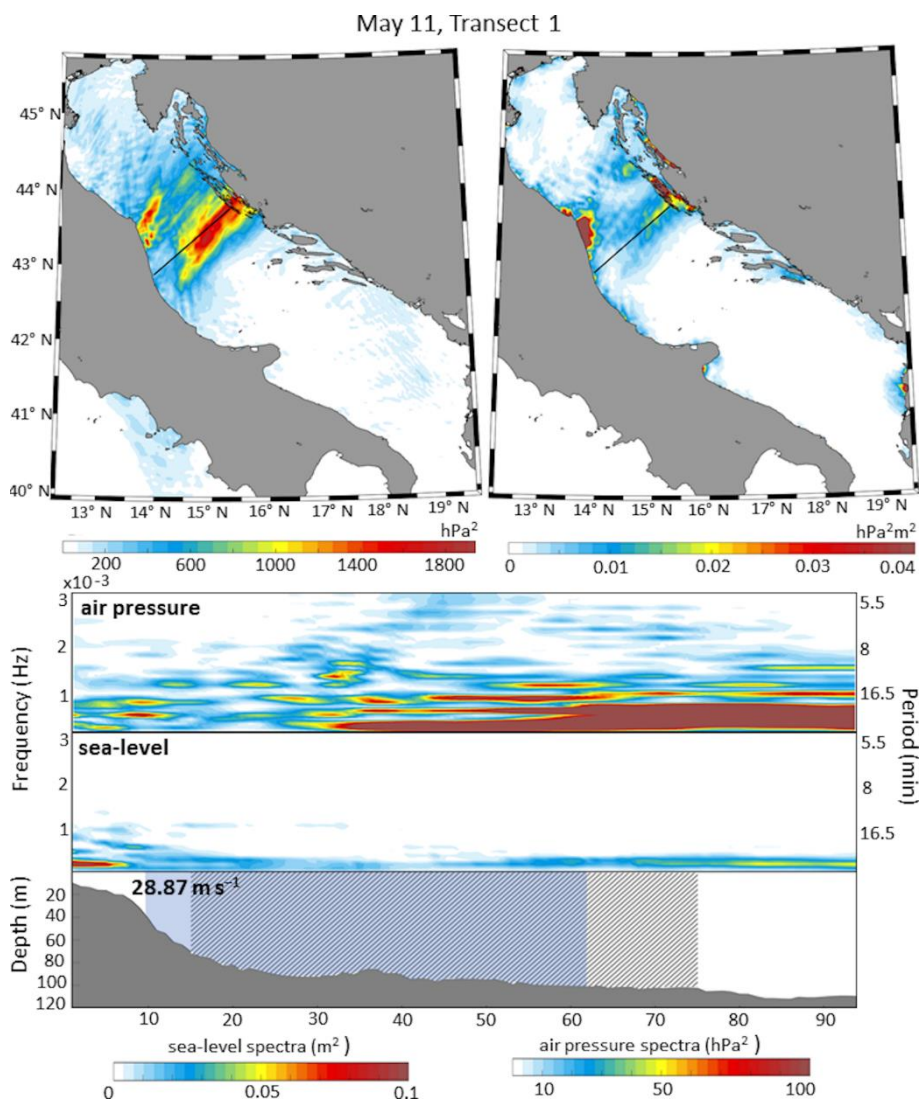
Figure 6: Meteotsunamigenic disturbance of the 11th of May 2020 along Transect 1. Air pressure spatial variance (top left panel) and transect sampling criteria (top right panel) have a mark of the selected transect containing meteotsunami energy banner (solid black line). Spectrograms of high-pass filtered mean sea-level air pressure (air pressure) and sea-level along the selected transect (middle panels) are conjoined by sections of the associated depth profile (bottom panel) where the Proudman resonance is likely to occur (shaded with diagonal stripes) and where the speed of the disturbance is calculated (in blue).
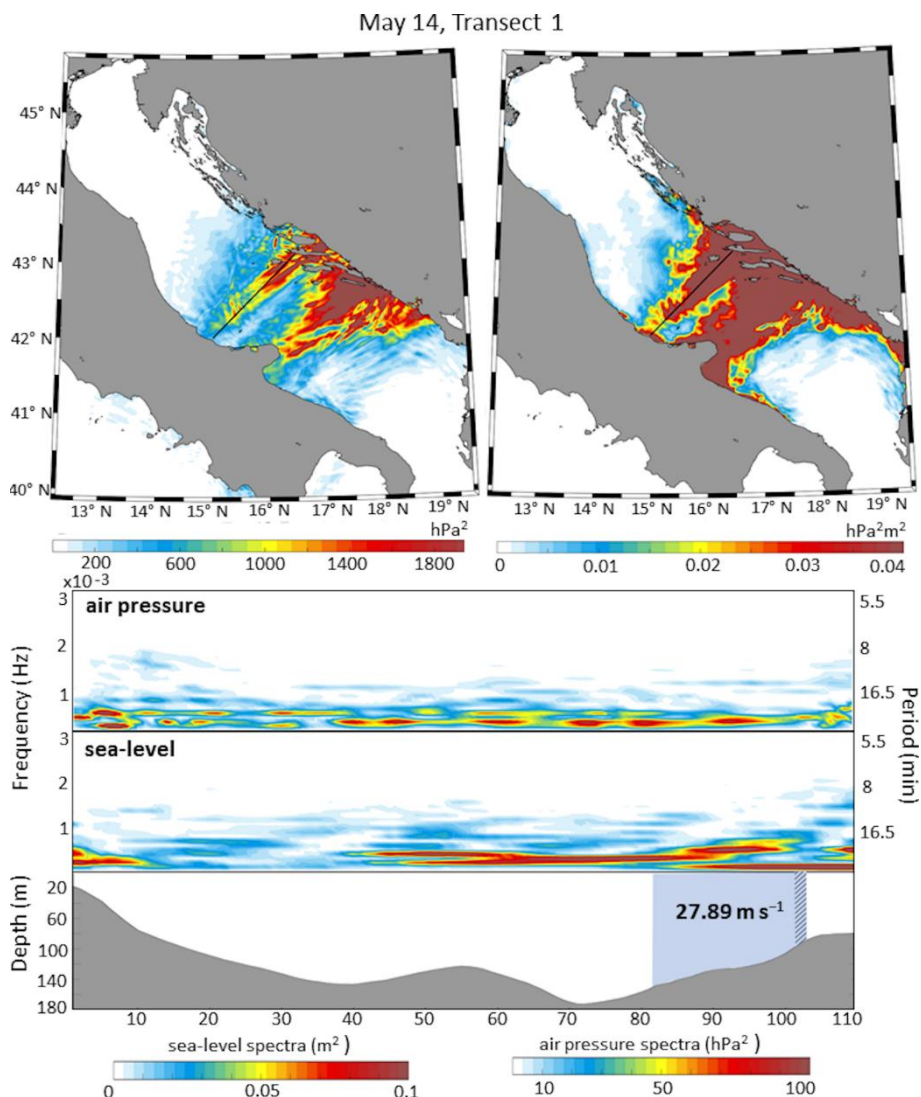
Figure 7: As in Fig. 6, but for the meteotsunamigenic disturbance of the 14th of May 2020 along Transect 1.

For the 14th of May, several modelled atmospheric disturbances are located in the middle Adriatic region (Figs. 7 and S4 to S6, left top panel). The location of the highest air pressure variances and the associated transect sampling criteria (top panels, Fig. 7), as well as the speed of the tracked most energetic disturbance of 27.9 m s⁻¹, makes this disturbance a good candidate for causing the meteotsunamis that flooded Vela Luka, Vrboska and Stari Grad harbours on this day. Nevertheless, the transect is in a deep water, and therefore the Proudman resonance is only likely to happen over a small part of the transect. Spectrograms show low energy for high frequencies both for atmosphere and ocean. Higher energies in the atmosphere, but not in the ocean, can be found on spectrograms of transects in Figs. S4 and S6. These disturbances are located too south or too north of the

domain to cause meteotsunamis in the harbours of interest. Also, the speeds of the tracked disturbances in Figs. S4 and S5 are

325   not within the range of speeds of meteotsunamigenic disturbances.
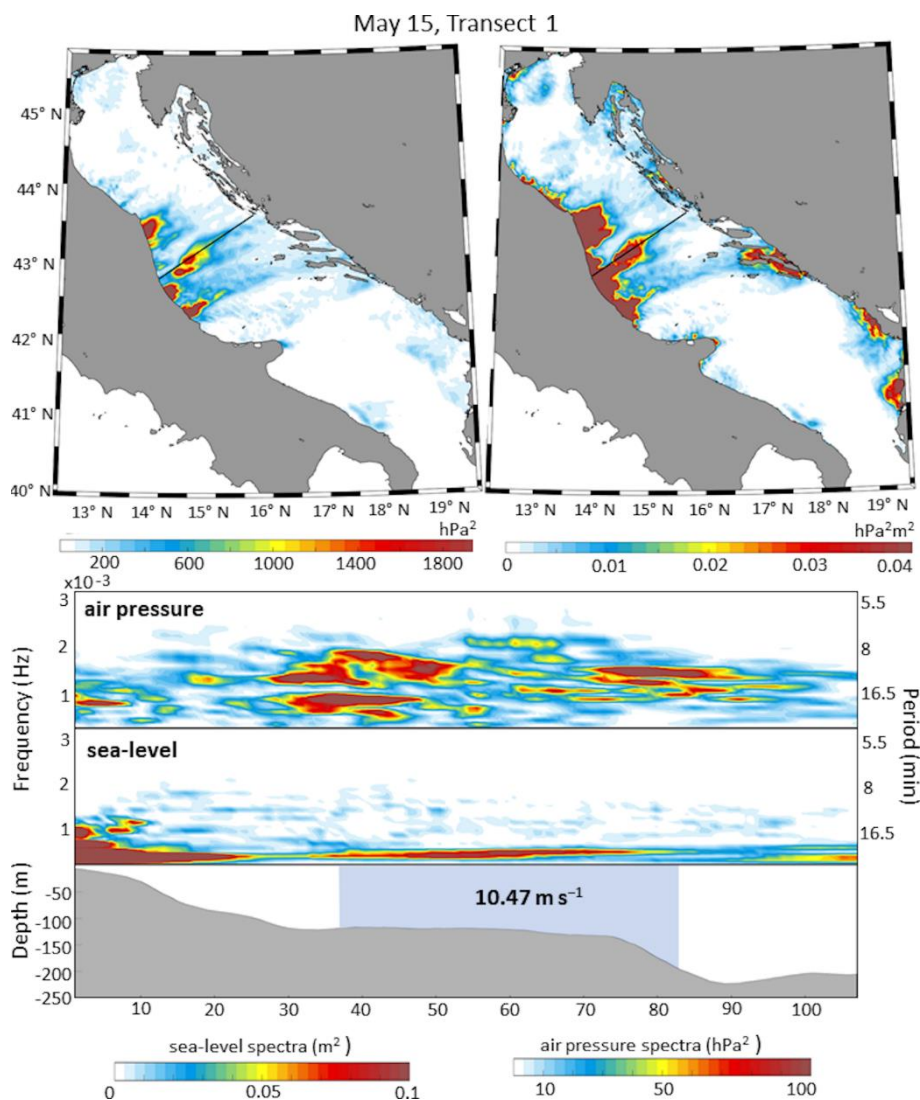
Figure 8: As in Fig. 6, but for the meteotsunamigenic disturbance of the 15th of May 2020 along Transect 1.

Two atmospheric disturbances are tracked for the 15th of May and presented in Figs. 8 and S7. The maximum in air pressure

variance (Fig. 8, left top panel) and the associated maximum in transect sampling criteria (Fig. 8, right top panel) are located

330   too northwest to cause the Vela Luka and Stari Grad flooding in the night of the 15th to 16th of May. Also, despite the high

energies in the atmosphere, no transfer to the sea can be seen along the transect, being restricted just near the coast. This is

probably due to the low speed of the disturbance (i.e. 10.5 m s^{-1}) and the depth (i.e. over 100 m) along the transect.

Spectrograms in Fig.S7 display high energies and strong ocean response at the beginning of the transect, but negligibly small

energy values on the rest of the transect, which is a good example of a dissipating disturbance. Low speed of the atmospheric

335 disturbance of only 11.6 m s⁻¹ and the lack of flat seabed could explain such a behaviour.
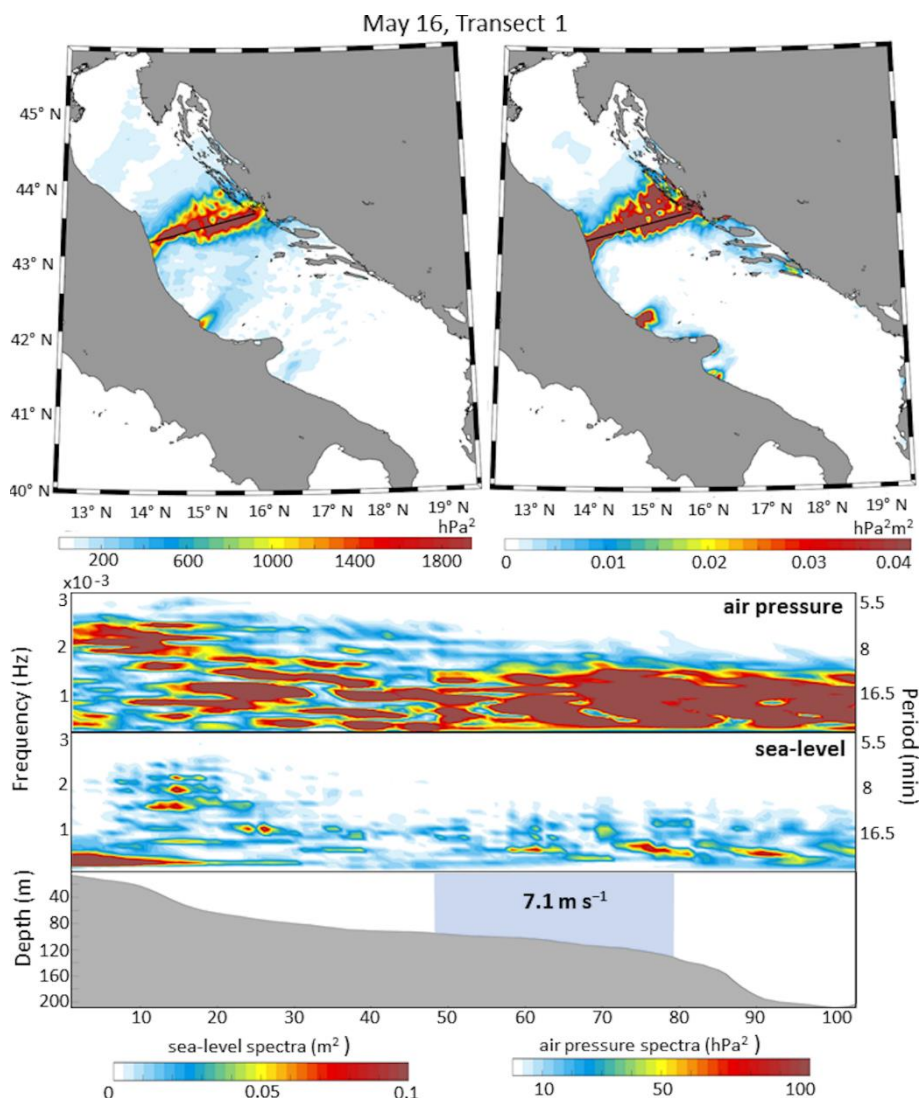
Figure 9: As in Fig. 6, but for the meteotsunamigenic disturbance of the 16ᵗʰ of May 2020 along Transect 1.

Three disturbances are analysed for 16ᵗʰ of May and presented in Figures 9, S8 and S9. Two northwestwardly shifted

atmospheric disturbances (Figs. 9 and S8) are extremely energetic and the transfer of energy to the sea is strong at the

340 beginnings of the transects. Speeds of the disturbances, of 7.1 m s⁻¹ and 11.3 m s⁻¹, are low compared to the normal speeds for

meteotsunamigenic disturbances. Southern disturbance (Fig. S9) has greater speed, of 25 m s⁻¹, but neither the atmosphere is

highly energetic nor the transfer of energy to the sea is strong anywhere but near the coast. This is displayed in both top panels,

and in spectrograms of Fig. S9. It should be noticed that the air-sea interaction is the strongest over the area where Proudman resonance is likely to happen.
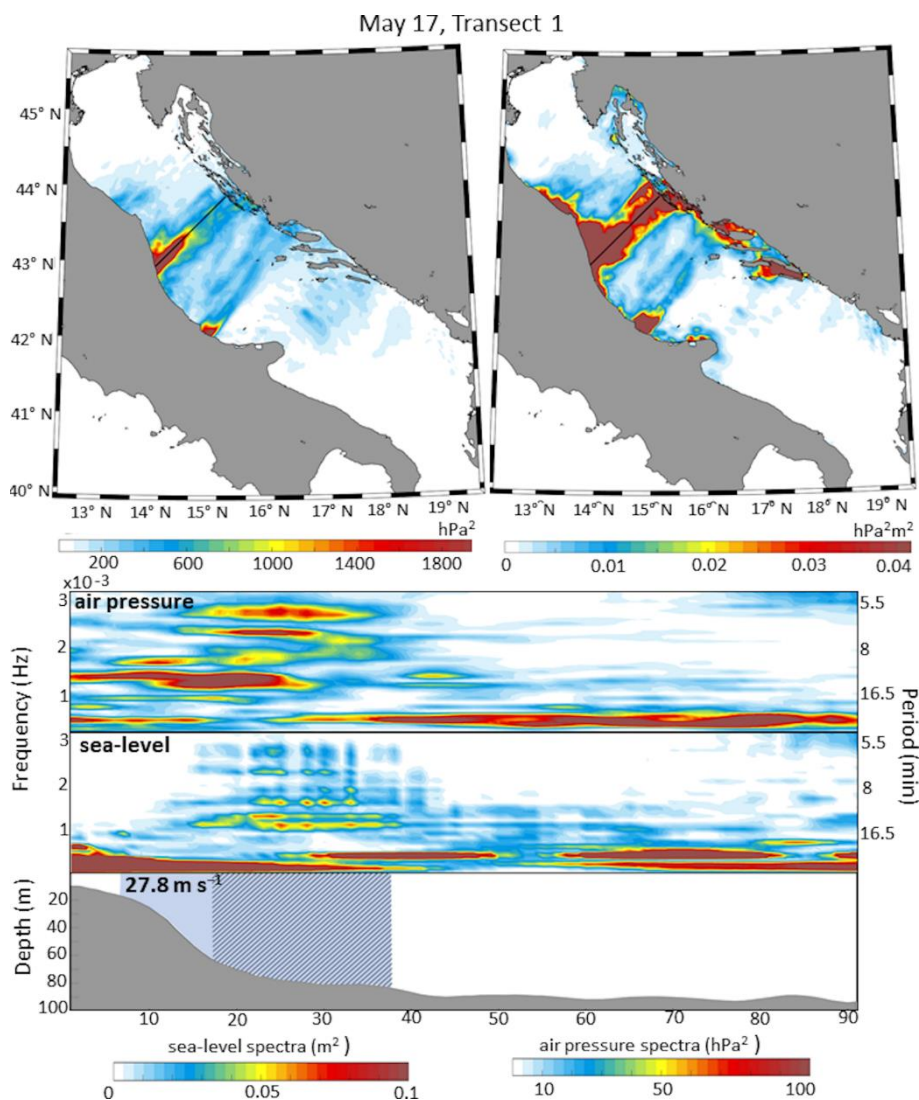
Figure 10: As in Fig. 6, but for the meteotsunamigenic disturbance of the 17th of May 2020 along Transect 1.

For the 17th of May, two of three modelled atmospheric disturbances (Figs. S10 and S11) are located where they could cause meteotsunamis along the eastern Adriatic coastline. However, the speeds of these disturbances, ranging from 10.3 m s^{-1} to 12.1 m s^{-1}, are too low and the atmosphere and the sea are not as energetic as they are over the transect analysed in Fig. 10. The atmosphere is extremely energetic over the selected transect and, since energy is well transferred to the ocean, high energies occurred for high frequencies in the ocean too. Spectrograms in Fig. 10 show that ocean's response to atmospheric disturbance

is pronounced over the whole transect, but is the strongest over the section which satisfied the Proudman resonance conditions. The disturbance travelled with 27.8 m s^{-1}, but as seen in top panels, it is again located in the northern part of middle Adriatic. For the 18th of May, the modelled atmospheric disturbances (Figs. S12 to S14) are crossing the middle Adriatic from southwest

355   to northeast, over the common path of meteotsunamigenic disturbances. Speeds of the tracked disturbances vary from 20.2 m s^{-1} to 30.3 m s^{-1}. Even though atmosphere is energetic for the transects presented in Figs. S12 and S14, the energy of the sea is not significantly higher for them than for the transect in Fig. S13, with low energy in the atmosphere. Therefore, despite the appropriate speeds and locations of the meteotsunamigenic disturbances, the energy is not well transferred from the atmosphere to the sea and no meteotsunami event is modelled.

360   For the 19th of May there is only one modelled disturbance, travelling at 19.4 m s^{-1} far south of the analysed region (Fig. S15). Energy content of both atmosphere and the sea is low for the selected transect, but some air-sea interactions are taking place in the eastern end of the transect (right top panel, Fig. S15).
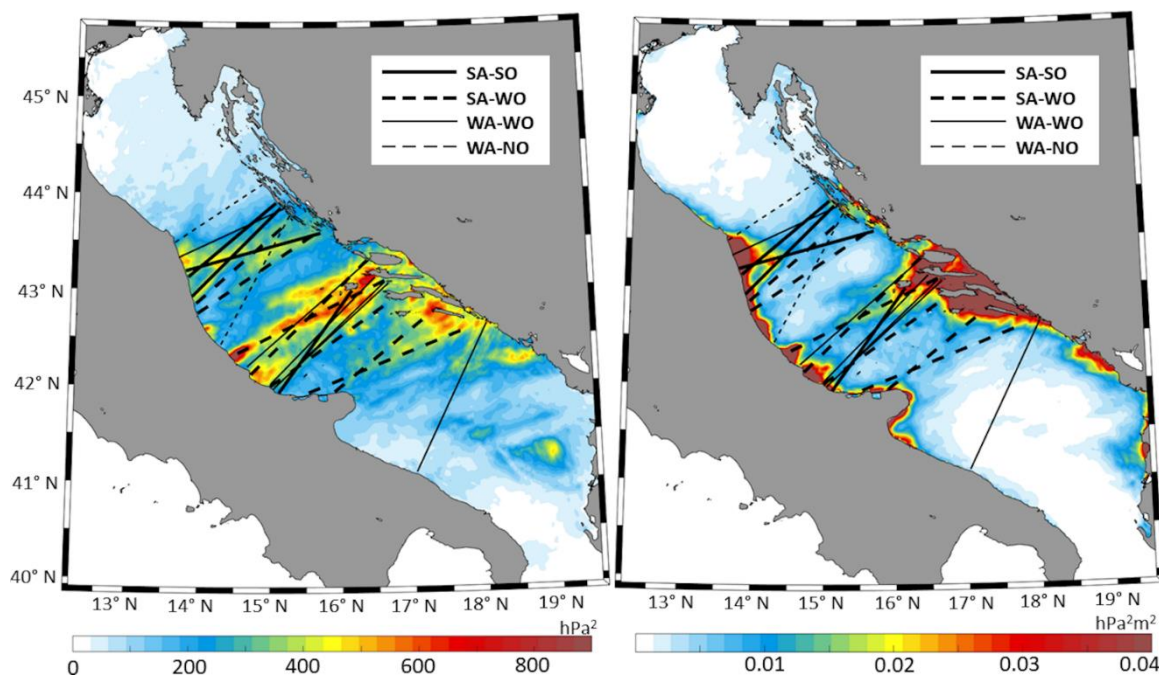
Figure 11: Averaged air pressure variances (left panel) and averaged transect sampling criteria (right panel) estimated for the
365   **ensemble of transects extracted between the 11th and 19th of May 2020. The modelled disturbances (black lines) are categorized depending on the strength of the atmospheric signal (SA for strong and WA for weak) and the ocean response (SO for strong, WO for weak, NO for none).**

Averaged air pressure variance and averaged transect sampling criteria derived from all the extracted transects between the 11th and 19th of May 2020 are presented in Fig.11, together with the selected transects. The transects are classified in four

370   different categories emphasizing the strength of the atmospheric disturbances as well as the energy transfer from the atmosphere to the ocean. The most intense atmospheric activity and air-sea interactions are located across the middle Adriatic

region. Additionally, despite relatively low averaged air pressure variances, the averaged values of the transect sampling criteria are the highest along the Dalmatian island and the middle Adriatic Italian coastlines. These results thus confirm that the intensity of the atmospheric disturbances is less important than the resonance – i.e. appropriate speed, period and depth along the transects (Denamiel et al., 2020) – and, of course, the bathymetry.

In brief, the presented results of the travelling air-sea meteotsunami energy banners show that the ocean model response to the atmospheric forcing highly depends on both the location and the frequency of the meteotsunamigenic disturbances, which are in our study often modelled too northwest of the most affected locations. Finally, the introduced transect sampling criteria does not seem to overall facilitate the decision-making process in terms of the transect selection. Indeed, even though for some events (e.g. Figs. 8, 9, 10) the new criterion highlights the strength of the air-sea interactions, these interactions are located along the same transects as captured by the highest values of the air pressure variance. As efficiency is important in early warning system, it can thus be concluded that the use of the ocean model results to better select the transect with maximum meteotsunami generation is not necessary in operational mode.

6 Stochastic hazard assessment

The analysis presented in previous sections has proven that the operational deterministic AdriSC model is not capable to properly reproduce the meteotsunami events of the 11-19 May 2020 period. However, parameters like location, amplitude, direction, speed, period, and width can be extracted from the atmospheric disturbances produced by the WRF 1.5-km model and used as inputs of the stochastic surrogate model. For the 11-19 May 2020 period (with the exception of the 12th and 13th), the stochastic surrogate model is thus run for Vela Luka, Stari Grad and Vrboska, with input variables from the atmospheric disturbances selected for each day along the transects presented in the previous section. The probabilities of the maximum elevation surpassing the flooding threshold are presented in Table 2.

Table 2. Meteotsunami hazard assessment derived with the stochastic surrogate model and provided as the probability of maximum sea elevation crossing the flooding thresholds in Vela Luka, Stari Grad and Vrboska during the 11-19 May 2020 period.

Location	\multicolumn{7}{c}{Probability of crossing the flooding threshold (%) during the 11-19 May 2020 multi-meteotsunami event}
	11th	14th	15th	16th	17th	18th	19th
Vela Luka	*16*	*10*	*19*	*14*	**10**	4	**34**
Stari Grad	*13*	2	*6*	*6*	4	1	9
Vrboska	*16*	*18*	**19**	**23**	**22**	3	**37**

Note: When the probabilities are above or equal to 10 % (highlighted in bold), the meteotsunami warning is triggered. In addition, probabilities at locations at which flooding has been reported by eyewitnesses during the events are highlighted in italics.

For the 11-19 May 2020 period when flooding and strong sea oscillations were reported for Vela Luka, Stari Grad and Vrboska (in italics, Table 2), the meteotsunami warning would have been triggered in Vela Luka and Vrboska for all the events, but

only for the 11th of May in Stari Grad. The results found in Stari Grad are, however, in good agreement with the moderate
400   oscillations (amplitude of 25-30 cm) of the high-pass filtered sea-levels extracted between the 14th and the 16th of May at the
tide gauge location. Additionally, the meteotsunami warning would have been wrongly triggered the 17th and the 19th in Vela
Luka and the 15th, 16th, 17th and 19th in Vrboska when no flooding was reported. It is worth noticing that, for the 17th and 19th
of May 2020, the forecasted meteotsunamigenic conditions capable to trigger the event mode of the CMeEWS are, in fact, in
good agreement with the strong air pressure oscillations observed along the western Adriatic coast (Fig. 1). Additionally, as
405   already shown in Denamiel et al. (2019b), false alarms are easily triggered in Vrboska. This may be linked to either the poor
representation of the Vrboska geomorphology within the ADCIRC model used to create the surrogate model or the choice of
the flooding threshold and therefore should be further investigated.

7 Summary and conclusions

In the Adriatic Sea, recurrent meteotsunami events are known to strongly impact the way of life of the coastal communities,
410   particularly in the Dalmatian islands where they can generate serious flooding. In this study, the capacity of the Croatian
meteotsunami early warning system (CMeEWS), which provides meteotsunami hazard assessments depending on the
deterministically forecasted and measured air pressure disturbances and the stochastically deduced maximum elevation
distributions derived with the surrogate model, is examined. As it is no longer operational, the capacity of the CMeEWS is
evaluated retroactively for the multi-event of the 11-19 May 2020. This event is of particular interest because
415   meteotsunamigenic synoptic patterns over the Adriatic were present during a prolonged period of about 5 to 10 days, not
previously observed for any meteotsunami. During this period, intense high-frequency air pressure and sea-level oscillations
were observed and recorded in the middle Adriatic with maximum sea-levels reached the 11th, 14th and 16th of May in Vela
Luka, Stari Grad and Vrboska.

One of the main originalities of this study is that the performances of the CMeEWS operational models – i.e. the WRF 1.5-km
420   atmospheric model and the ADCIRC ocean model from the AdriSC modelling suite – are assessed via energy banners. Analysis
of composites of frequency-time spectrograms has shown that the deterministic models are generally not capable to reproduce
the meteotsunami events in affected bays but can produce strong meteotsunamigenic disturbances often shifted north-westward
from them. Results of the analysis of selected travelling air-sea energy banners led to the conclusion that sea-level response is
not only governed by the Proudman resonance but also by other processes such as the interactions with the complex bathymetry
425   present off the affected bays. It was demonstrated that, even though the strongest atmospheric activity was modelled in the
middle Adriatic along common air pressure disturbance pathways, the meteotsunami events were always missed by the
ADCIRC ocean model at Vela Luka and Stari Grad during the 11-19 May 2020 period. This most probably indicates that the
frequency of the air pressure disturbances is not properly reproduced by the WRF 1.5-km model, posing a question of
appropriateness of the state-of-the-art atmospheric models in terms of their resolution and setup (Horvath and Vilibić, 2014).
430   Finally, this study also highlighted that using the ocean model results in combination with the atmospheric model results with

the so-called transect sampling criteria is not helping to improve the selection of atmospheric conditions needed to feed the stochastic meteotsunami surrogate model. However, due to the systematic error link to the shift of the disturbances towards the north, it may be envisioned in the future to apply a correction concerning the start point location before using the surrogate model.

435 Given these results, the following question can be raised: should the ADCIRC ocean model be run in operational mode within the CMeEWS or should the meteotsunami hazard assessments be derived solely with the stochastic surrogate model? In the presented case, as deterministic ocean model fails for all events, the question is easily answered. And, in general, due to the uncertainties associated with operational modelling of meteotsunamigenic disturbances, the stochastic approach has proven to be an optimal option. Nevertheless, the ADCIRC ocean model can still be used for other hazards such as extreme storm surges

440 associated with wind-waves and not only for meteotsunami events.

Concerning the evaluation of the stochastic model fed by the extracted meteotsunamigenic air pressure conditions along the selected transects, in most of the cases and despite some false alarms, the coastal communities of Vela Luka, Stari Grad and Vrboska would have been warned of potential meteotsunami events if the CMeEWS had been operational. Even though warning effectiveness highly depends on the resident trust which can be easily eroded from false alarms and/or missed events,

445 the uncertainty faced by the Croatian coastal communities during the 11-19 May 2020 period and reported by several local newspapers, is probably far worst. The meteotsunami surrogate model, even if not perfect as not including the storm surges in Stari Grad for example, has thus been proven to be extremely useful and reliable during this multi-meteotsunami event.

To conclude, as operational models often fail to properly forecast extreme events, the continuous development of stochastic approaches – such as the meteotsunami surrogate model within the CMeEWS – should be an avenue explored by the extreme

450 sea-level community in order to improve early warning systems.

Code availability

Codes of COAWST, WRF and ADCIRC models, can be obtained on the following links: https://www.usgs.gov/software/coupled-ocean-atmosphere-wave-sediment-transport-coawst-modeling-system, https://www2.mmm.ucar.edu/wrf/users/downloads.html, http://adcirc.org/.

455 **Data availability**

The model results and the measurements used to produce this article can be obtained under the Open Science Framework (OSF) FAIR data repository https://osf.io/24m8e/ (doi: 10.17605/OSF.IO/24M8E).

Author contributions

IV and CD defined concept and design of the study. Material preparation was done by CD and IT. Set-up of the model and
460   simulations were performed by CD and IT. Production of the figures was done by CD and IT. Analysis of the results was
performed by IV, CD and IT. The first draft of the manuscript was written by IT. All authors were engaged in commenting,
revising and polishing of the manuscript. All authors read and approved the final manuscript.

Competing interests

The authors declare that they have no conflict of interest.

465   **Acknowledgements**

Special thanks are given for the support of the European Centre for Middle-range Weather Forecast (ECMWF) staff, in
particular Xavier Abellan and Carsten Maass, as well as for ECMWF's computing and archive facilities used in this research.
This work has been supported by projects ADIOS (Croatian Science Foundation Grant IP-2016-06-1955), BivACME (Croatian
Science Foundation Grant IP-2019-04-8542), CHANGE WE CARE (Interreg Croatia-Italy program) and ECMWF Special
470   Project (The Adriatic decadal and inter-annual oscillations: modelling component).

References

Anderson, E.J., and Mann, G.E.: A high-amplitude atmospheric inertia–gravity wave-induced meteotsunami in Lake Michigan,
Nat. Hazards, https://doi.org/10.1007/s11069-020-04195-2, 2020.

Belušić, D., Grisogono, B., and Klaić, Z.B.: Atmospheric origin of the devastating coupled air–sea event in the east Adriatic,
475   J. Geophys. Res. Atm., 112, D17111. https://doi.org/10.1029/2006JD008204, 2007.

Denamiel, C., Šepić, J., and Vilibić, I.: Impact of geomorphological changes to harbour resonance during meteotsunamis: The
Vela Luka Bay test case, Pure Appl. Geophys., 175, 3839–3859, https://doi.org/10.1007/s00024-018-1862-5, 2018.

Denamiel, C., Šepić, J., Ivanković, D., and Vilibić, I.: The Adriatic Sea and Coast modelling suite: Evaluation of the
meteotsunami forecast component, Ocean Model., 135, 71–93, https://doi:10.1016/j.ocemod.2019.02.003, 2019a.

480   Denamiel, C., Šepić, J., Huan, X., Bolzer, C., and Vilibić, I.: Stochastic surrogate model for meteotsunami early warning
system in the eastern Adriatic Sea, J. Geophys. Res. Oceans, 124, 8485-8499, https://doi.org/10.1029/2019JC015574, 2019b.

Denamiel, C., Huan, X., Šepić, J., and Vilibić, I.: Uncertainty propagation using polynomial chaos expansions for extreme sea-
level hazard assessment: The case of the eastern Adriatic meteotsunamis, J. Phys. Oceanogr., 50, 1005–1021,
https://doi.org/10.1175/JPO-D-19-0147.1, 2020.

485   Ewing, M., Press, F., and Donn, W. L.: An explanation of the Lake Michigan wave of 26 June 1954, Science, 120, 684–686, https://doi:10.1126/science.120.3122.684, 1954.

Hersbach, H., Bell, B., Berrisford, P., Hirahara, S., Horányi, A., Muñoz-Sabater, J., Nicolas, J., Peubey, C., Radu, R., Schepers, D., Simmons, A., Soci, C., Abdalla, S., Abellan, X., Balsamo, G., Bechtold, P., Biavati, G., Bidlot, J., Bonavita, M., De Chiara, G., Dahlgren, P., Dee, D., Diamantakis, M., Dragani, R., Flemming, J., Forbes, R., Fuentes, M., Geer, A., Haimberger, L.,

490   Healy, S., Hogan, R.J., Hólm, E., Janisková, M., Keeley, S., Laloyaux, P., Lopez, P., Lupu, C., Radnoti, G., de Rosnay, P., Rozum, I., Vamborg, F., Villaume, S., and Thépaut, J.-N.: The ERA5 Global Reanalysis, Q. J. Roy. Meteorol. Soc., 146, 1999–2049, https://doi.org/10.1002/qj.3803, 2020.

Hibiya, T., and Kajiura, K.: Origin of the Abiki phenomenon (a kind of seiche) in Nagasaki Bay, J. Oceanogr. Soc. Jpn., 38, 172–182, https://doi:10.1007/BF02110288, 1982.

495   Horvath, K., and Vilibić, I.: Atmospheric mesoscale conditions during the Boothbay meteotsunami: a numerical sensitivity study using a high-resolution mesoscale model, Nat. Hazards, 74, 55-74, https://doi.org/10.1007/s11069-014-1055-1, 2014.

Jansà, A., and Ramis, C.: The Balearic rissaga: from pioneering research to present-day knowledge. Nat. Hazards, https://doi.org/10.1007/s11069-020-04221-3, 2020.

Jansà, A., Monserrat, S., and Gomis, D.: The rissaga of 15 June 2006 in Ciutadella (Menorca), a meteorological tsunami, Adv.

500   Geosci., 12, 1–4, https://doi.org/10.5194/adgeo-12-1-2007, 2007.

Linares, A., Wu, C. H., Bechle, A. J., Anderson, E. J., and Kristovich, D. A. R.: Unexpected rip currents induced by a meteotsunami, Sci. Rep., 9, 2105, https://doi:10.1038/s41598-019-38716-2, 2019.

Lindzen, R.S., and Tung K.-K.: Banded convective activity and ducted gravity waves, Mon. Weather Rev., 104, 1602–1617, https ://doi.org/10.1029/2018J D0295 23, 1976.

505   Luettich, R.A., Birkhahn, R.H., and Westerink, J.J.: Application of ADCIRC-2DDI to Masonboro Inlet, North Carolina: A brief numerical modeling study. Contractors Report to the US Army Engineer Waterways Experiment Station, August, 1991.

Miles, J., Munk, W.: Harbour paradox, J. Waterw. Harbour. Div. ASCE, 87, 111–132, 1961.

Monserrat, S., and Thorpe, A.J.: Gravity-wave observations using an array of microbarographs in the Balearic Islands, Q. J. Roy. Meteorol. Soc., 118, 259–282. https ://doi.org/10.1002/qj.49711 85040 5, 1992.

510   Monserrat, S., and Thorpe, A.J.: Use of ducting theory in an observed case of gravity waves, J. Atmos. Sci., 53, 1724–1736, https://doi.org/10.1175/1520-0469(1996)053%3c1724:UODTIA%3e2.0.CO;2, 1996.

Monserrat, S., Vilibić, I., and Rabinovich, A.B.: Meteotsunamis: atmospherically induced destructive ocean waves in the tsunami frequency band, Nat. Hazards Earth Syst. Sci., 6, 1035-1051, https://doi.org/10.5194/nhess-6-1035-2006, 2006.

Neumann, B., Vafeidis, A. T., Zimmermann, J., and Nicholls, R. J.: Future coastal population growth and exposure to sea-

515   level rise and coastal flooding - A global assessment, PLoS ONE, 10, e0118571, https://doi.org/10.1371/journal.pone.0118571, 2015.

Nicholls, R. J., and Cazenave, A.: Sea-level rise and its impact on coastal zones, Science, 328, 1517-1520, https://doi.org/10.1126/science.1185782, 2010.

Orlić, M., Belušić, D., Janeković, I., and Pasarić, M.: Fresh evidence relating the great Adriatic surge of 21 June 1978 to
520 mesoscale atmospheric forcing, J. Geophys. Res. Oceans, 115, C06011, https://doi.org/10.1029/2009JC005777, 2010.

Pattiaratchi, C.B., and Wijeratne, E.M.S.: Are meteotsunamis an underrated hazard?, Philos. Trans. R. Soc. A, 373, 20140377.
https://doi.org/10.1098/rsta.2014.0377, 2015.

Pinardi, N., Allen, I., Demirov, E., De Mey, P., Korres, G., Lascaratos, A., Le Traon, P-Y., Maillard, C., Manzella, G., and
Tziavos C.: The Mediterranean ocean Forecasting System: first phase of implementation (1998-2001), Ann. Geophys., 21, 3-
525 20, https://doi:10.5194/angeo-21-3-2003, 2003.

Proudman, J.: The effects on the sea of changes in atmospheric pressure, Mon. Not. R. Astron. Soc. Geophys. Suppl., 2, 197–
209, https://doi.org/10.1111/j.1365-246X.1929.tb05408.x, 1929.

Rabinovich, A.B.: Seiches and harbour oscillations. In: Kim YC (eds) Handbook of coastal and ocean engineering, pp 193–
236. World Scientific, Singapore. https://doi.org/10.1142/9789812819307_0009, 2009.

530 Rabinovich, A.B.: Twenty-seven years of progress in the science of meteorological tsunamis following the 1992 Daytona
Beach event. Pure Appl. Geophys., 177, 1193–1230, https://doi.org/10.1007/s0002 4-019-02349 -3, 2020.

Renault, L., Vizoso, G., Jansà, A., Wilkin, J., and Tintoré, J.: Toward the predictability of meteotsunamis in the Balearic Sea
using regional nested atmosphere and ocean models, Geophys. Res. Lett., 38, L10601, https://doi:10.1029/2011gl047361,
2011.

535 Salaree, A., Mansouri, R., and Okal, E. A.: The intriguing tsunami of 19 March 2017 at Bandar Dayyer, Iran: field survey and
simulations, Nat. Hazards, 90, 1277–1307, https://doi: 10.1007/s11069-017-3119-5, 2018.

Soize, C., and Ghanem, R. G.: Physical systems with random uncertainties: Chaos representations with arbitrary probability
measure, SIAM J. Sci. Comp., 26(2), 395–410, https://doi.org/10.1137/S1064827503424505, 2004.

Šepić, J., Vilibić, I., and Belušić, D.: The source of the 2007 Ist meteotsunami (Adriatic Sea), J. Geophys. Res. Oceans, 114,
540 C03016, doi:10.1029/2008JC005092, 2009.

Šepić, J., Vilibić, I., and Strelec Mahović, N.: Northern Adriatic meteorological tsunamis: Observations, link to the atmosphere,
and predictability, J. Geophys. Res., 117, C02002, https://doi.org/10.1029/2011JC007608, 2012.

Šepić, J., Vilibić, I., Rabinovich, A., and Monserrat, S.: Widespread tsunami-like waves of 23-27 June in the Mediterranean
and Black Seas generated by high-altitude atmospheric forcing, Sci. Rep., 5, 11682, https://doi.org/10.1038/srep11682, 2015.

545 Skamarock, W. C., Klemp, J. B., Dudhia, J., Gill, D. O., Barker, D. M., Wang, W., and Powers, J. G.: A Description of the
Advanced Research WRF Version 2. NCAR Technical Note NCAR/TN-468+STR, https://doi:10.5065/D6DZ069T, 2005.

Vilibić, I., Domijan, N., Orlić, M., Leder, N., and Pasarić, M.: Resonant coupling of a traveling air-pressure disturbance with
the east Adriatic coastal waters. J. Geophys. Res. Oceans, 109, C10001, https://doi.org/10.1029/2004JC002279, 2004.

Vilibić, I., Monserrat, S., Rabinovich, A., and Mihanović, H.: Numerical modelling of the destructive meteotsunami of 15
550 June, 2006 on the coast of the Balearic Islands, Pure Appl. Geophys., 165, 2169–2195, https://doi.org/10.1007/s00024-008-
0426-5, 2008.

Vilibić, I., Šepić, J., Rabinovich, A.B.. and Monserrat, S.: Modern approaches in meteotsunami research and early warning, Front. Mar. Sci., 3, 57, https://doi.org/10.3389/fmars.2016.00057, 2016.

Vučetić, T., Vilibić, I., Tinti, S., and Maramai, A.: The Great Adriatic flood of 21 June 1978 revisited: An overview of the

555 reports, Phys. Chem. Earth, 34, 894-903, https://doi.org/10.1016/j.pce.2009.08.005, 2009.

Warner, J. C., Armstrong, B., He, R., and Zambon, J. B.: Development of a Coupled Ocean-Atmosphere-Wave-Sediment Transport (COAWST) modeling system, Ocean Modell., 35, 230-244, https://doi.org/10.1016/j.ocemod.2010.07.010, 2010.

Xiu, D., and Karniadakis, G. E.: The Wiener–Askey polynomial chaos for stochastic differential equations, SIAM J. Sci. Comp., 24(2), 619–644, https://doi.org/10.1137/S1064827501387826, 2002.

560 Zemunik, P., Bonanno, A., Mazzola, S., Giacalone, G., Fontana, I., Genovese, S., Basilone, G., Candela, J., Šepić, J., Vilibić, I., and Aronica, S.: Observing meteotsunamis ("Marrobbio") in the southwestern coast of Sicily, Nat. Hazards, https://doi.org/10.1007/s11069-020-04303-2, 2020.

Zsótér, E., Pappenberger, F., and Richardson, D.: Sensitivity of model climate to sampling configurations and the impact on the Extreme Forecast Index. Meteorol. Appl., 22, 236–257. https://doi.org/10.1002/met.1447, 2014.

565